EXPERIMENTS WITH AN OPTICAL SEISMOMETER

Mark Zumberge, Jonathan Berger, and José Otero; *Scripps Institution of Oceanography, University of California, San Diego* Erhard Wielandt; *Institute of Geophysics, Stuttgart University, Stuttgart, Germany*

ABSTRACT

Modern seismometers rely on electronic displacement transducers to sense the motion of an inertial mass suspended by a spring. The more sophisticated systems use electrostatic or electromagnetic force-feedback on the inertial mass to ameliorate the shortcomings of the spring and the displacement transducer.

Recent advances in optical fiber technology and digital signal processing offer an alternative to the modern observatory seismometer. We have recently developed an optical fringe resolver to replace the electronic displacement transducer that promises to lead to a greatly improved seismometer. The use of optical fiber interferometry in place of electronics adds other important benefits, including immunity to noise pickup, simplification of remote deployment (in a borehole, for example), the elimination of a heat source in the seismometer—an important cause of noise in the best existing systems, and elimination of electrical connections between the seismometer and the recording system.

Our first test of this concept was to apply it to a standard STS-1 seismometer. For this experiment, we added interferometric components to the seismometer frame and a retroreflector to the seismometer's mass. We removed the feedback electronics and recorded the STS-1 mass displacement with our new interferometric system. Simultaneously we recorded the output of a standard STS-1 set up on the same pier. The results, which include observations of large teleseisms and microseisms, indicate that the new technique is promising. In our second experiment, we measured the inherent noise floor of the displacement transducer. In a 100 Hz bandwidth, the RMS noise was approximately 5×10^{-12} m. This, when applied to a mass-spring suspension having a 5.4 s period and a Q of 7.4 will resolve the USGS ground noise model up to at least 15 Hz.

The use of optical fiber interferometry rather than traditional electronic displacement transducers affords significant advantages, including:

- ∑A linear, high-resolution displacement detector — the proposed optical sensor includes the functionality of a digitizer providing about a 30-bit digital output;
- ∑Absolute displacement measurement referenced to the wavelength of light;
- ∑Bandwidth sufficient to resolve the USGS Low Noise Model from DC to > 15 Hz;
- ∑Dynamic range sufficient to record the largest teleseisms and most regional and local earthquakes;
- ∑Minimum electronics in package - only optical fiber connection to the seismometer, minimizing heat from electronics in the sensor package and noise pickup from connecting electrical cables;
- ∑Smaller package — our design will be applicable to both vault and borehole installations and should be relatively easy to manufacture.

IRIS Design Goals

- Clip level of 5.8×10^{-3} m s^{-1} RMS over the band 10^{-4} Hz to 15 Hz.
- Bandwidth of 10^{-4} Hz to about 15 Hz.
- Seismometer linearity of 90 dB or greater.
- Calibrations good to 1% and gain stability of 1% between calibrations.
- Sensitive axis orientation accurate to 0.6° (minimum).

We believe that our new design will substantially meet most if not all these goals. At the very least, the design will offer an alternative to the existing very-broadband seismometers.

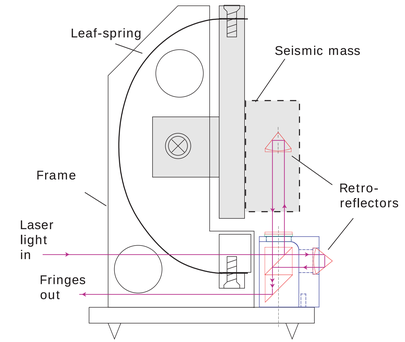

Figure 1. Conceptual mechanical design for vertical component Optical Seismometer.

Design Considerations

- The amplitudes of the displacements to be measured are quite challenging – ambient ground noise at a quiet site can be as small as 10^{-12} m Hz$^{-1/2}$ at 10 Hz.
- The free period T, the ground acceleration Δg at frequency f and the displacement Δx are related by:

$$\Delta g = \Delta x \frac{4\pi^2}{T^2}\left[\left((fT)^2-1\right)^2+\left(fT/Q\right)^2\right] \xrightarrow{f\to 0} \Delta x \frac{4\pi^2}{T^2} \qquad (1)$$

where Q is the mechanical quality factor. For a non-feedback system, equation (1) shows that the ratio of mass displacement to applied acceleration (force) is a function of the free period and Q of the suspension.

- A mass of 0.1 to 0.3 kg and a free period of 3 to 5 s is achievable in a 10 cm package. Brownian noise considerations require $MTQ > 1$ kg s. A leaf-spring geometry provides the required free period.
- Observatory-grade seismometers employ a displacement transducer such as a linear variable differential transformer or a variable capacitive sensor. These have difficulties in resolving required displacements (their self noise limits the bandwidth) while producing a linear output and also have very limited dynamic range.
- We have developed an optical displacement transducer that promises to lead to a greatly improved seismometer. The use of optical fiber interferometry (described below) in place of electronics adds other important benefits, including immunity to noise pickup, simplification of remote deployment (in a borehole, for example), the elimination of a heat source in the seismometer—an important cause of noise in the best existing systems, and the elimination of components that can be damaged in electrical storms (a problem in many field settings).

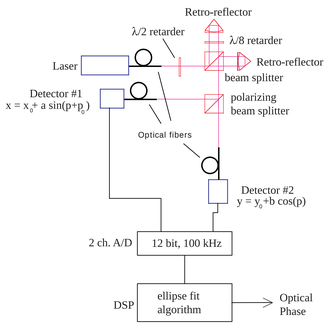

Figure 2 shows a simple Michelson interferometer modified to produce two fringe signals that are in quadrature. A birefringent element (a λ/8 phase retarder) in one of the two arms lengthens the optical path for one polarization by λ/4 in one round trip. Illuminating the interferometer with both polarizations (by adjustment of a λ/2 phase retarder before the beamsplitter) and separating the two fringe signals with a polarizing beamsplitter produces the sine and cosine components of the optical phase difference. The two-photodetector output voltages vary while the optical path difference L changes as shown in Figure 3a.

Optical Fringe Resolver

- For seismometry, we require resolution in displacement of about 10^{-12} m Hz$^{-1/2}$ at 10 Hz, and the ability to follow displacements that span several mm.
- We have developed and tested a digital-signal-processor (DSP) based fringe resolver with a demonstrated resolution of 5×10^{-13} m Hz$^{-1/2}$ at 1 Hz and higher.
- Optical fibers allow us to move the laser and two detectors far away from the interferometer (the optical fibers after the laser and in front of the detectors in Figure 2 can be hundreds of meters in length, if required). Because the optical path difference sensed by the interferometer is in free-space outside of the fibers, the optical path lengths of the fibers themselves are unimportant.

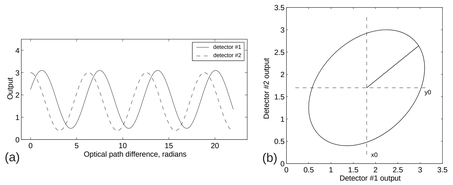

Figure 3. The quadrature fringe signals. In (a) we plot the two signals vs. time. In (b) we plot x and y against each other which yields an ellipse. Increasing (decreasing) the path length difference causes the x-y ordered pair at any instant to move clockwise (counterclockwise) around the ellipse. It is this position on the ellipse that we want to record.

Fringe Resolver Specifications

- 12-bit, 100k samples per second analog-to-digital converter interfaced directly to a DSP
- Full Scale - 10 mm displacement and 1.5×10^{-2} m s^{-1} velocity
- Present electronics capable of 500k samples per second, making the full-scale velocity 7.5×10^{-2} m s^{-1}
- Phase determined at 100k sps and filtered to 200 sps. Phase resolution at 200 sps frequency is better than 9×10^{-5} radian.
- Measured optical fringe resolver noise floor: 5×10^{-13} m Hz$^{-1/2}$.
- Pre-prototype optical fiber interferometer can resolve the USGS Low Noise Model ground noise from DC to about 15 Hz.

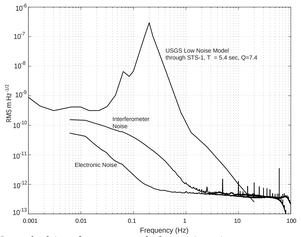

Figure 4. Smoothed interferometer and electronic noise spectra compared with the USGS Low Noise Model acceleration spectrum passed through Equation (1) with T= 5.4 seconds and Q = 7.4, which corresponds to the STS-1. Spikes in the spectra are believed to be an artifact of the fringe-processing scheme.

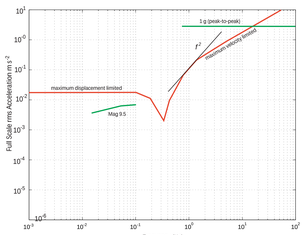

Figure 5. There are two limits to the new design. First, the mass stops limit mass motion to about ± 1 cm. Second, the optical fringe resolver will lose track of the mass when the velocity exceeds 7.5 cm/s. The red curve shows how these limits translate to large accelerations (examples of which are shown with the green curves) with our prototype suspension.

Pre-Prototype: A Modified STS-1

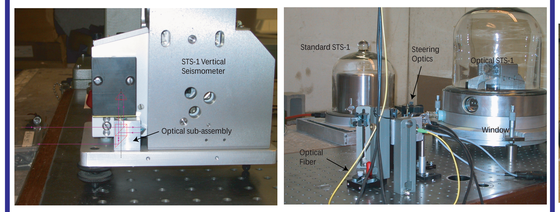

Figure 6. Photographs of the experiment we carried out comparing a standard STS-1 to one in which we replaced the electronics with optics. Both seismometers were situated on the same pier. The first was operated normally. In the second, the electronic position sensor was disconnected, and the forcing coil was shorted internally to provide damping. No electrical connections were made to the modified STS-1; laser light entered and exited through a window in the seismometer's vacuum jar to provide the position information.

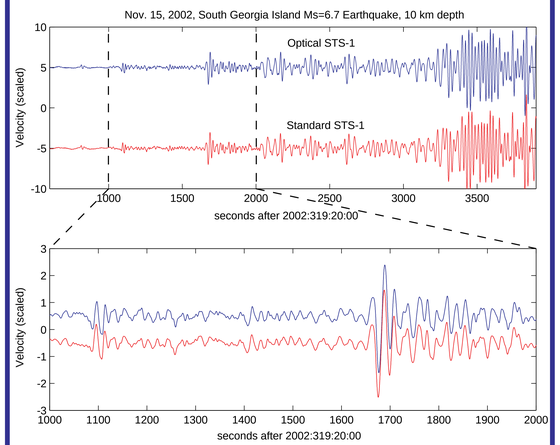

Figure 7. Seismograms recorded with both the modified Optical STS-1 and a standard STS-1 from a magnitude 6.7 event off South Georgia Island on 15 Nov. 2002 (about 115° away from San Diego). The signal at IGPP reached an amplitude of $\pm 2.5 \times 10^{-4}$ m of mass motion, very close to the clip level of the STS-1 seismometer but well within the dynamic range of the Optical Seismometer.

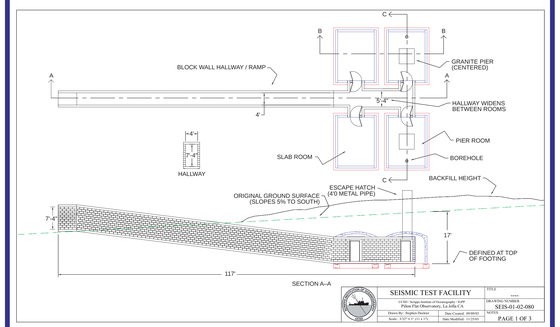

Figure 8. We have new facilities to test the prototype seismometer. We have precision laboratory shake tables in our lab, and we are constructing an underground seismic test vault at Piñon Flat Observatory.

Prototype Vertical Component Optical Seismometer

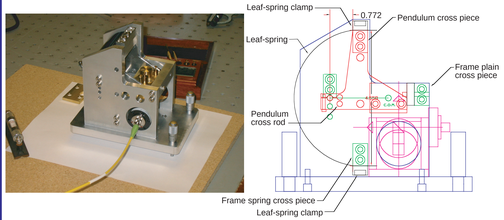

Figure 9. Prototype Vertical Optical Seismometer. This unit has a mass of 360 grams and a free period of a few seconds. The spring is a single strip of "NiSpan-C", a trade name for a particular alloy of iron-nickel with small amounts of chromium and titanium.

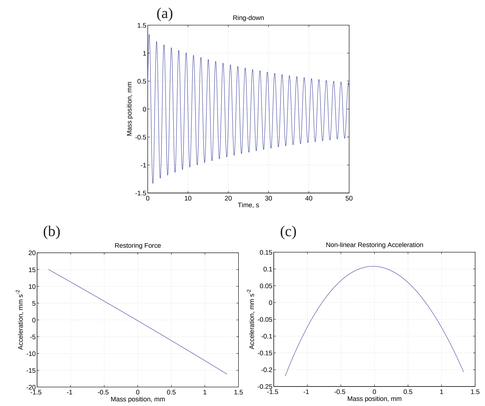

Figure 10. (a) displays the ring-down of the prototype vertical seismometer. The shape of the curve is governed by the damping and the restoring force of the spring. Numerically correlating the computed acceleration with position yields the spring constant; correlating acceleration with velocity yields the damping. (b) shows the restoring force (after correcting for damping) as a function of mass position. The slope of this is the spring constant k over the mass m; period $T = 2\pi(m/k)^{1/2}$. (c) shows the non-linear portion that results from the geometry of the leaf-spring suspension.

Because we are not using force feedback, we must solve the problems of non-linearity and cross-coupling. There are two sources of non-linearity in the instrument described here:

- The displacement transducer tracks the mass's motion along the optical axis when in fact the mass moves in an arc
- The restoring force does not follow exactly Hooke's law; there are higher order terms

Because the mass moves in an arc, when it is away from the equilibrium position, its sensitive axis changes slightly resulting in cross-coupling.

Normally, the differential equation which governs a seismometer suspension is

$$m\ddot{z} + r\dot{z} + kz = -m\ddot{h}$$

where m is the seismometer mass, z is the mass position w.r.t. the frame, r is the drag coefficient, k the spring constant, and h is the ground position. With the new system, this must be modified to:

$$m\ddot{z}_C + r\dot{z}_C + k_1 z_C + k_2 z_C^2 + \ldots = -m\ddot{h} + \alpha(z_C)\ddot{n}$$

where z_C is the position corrected for the arc motion, α is the cross-coupling coefficient, and n is the ground displacement normal to the sensitive axis. The displacement is computed by a DSP; it will be fairly straightforward to further develop the DSP code to correct for non-linearity and cross-coupling.